FIFTH AUSTRALASIAN CONFERENCE

on

HYDRAULICS AND FLUID MECHANICS

at

University of Canterbury, Christchurch, New Zealand

1974 December 9 to December 13

A Numerical Study of an Axisymmetric Heat Island

by

Peter G. Williams

SUMMARY

Some aspects of convective dynamics over compact urban areas can be studied in a simple axisymmetric "heat island" model. The numerical model described in this paper explores motion over a low intensity circular heat source in an extensive horizontal boundary, under conditions of very light external winds and a strong inversion; results are presented to show the dependence of motion on (I) the flow Rayleigh number, (II) the various boundary conditions, (III) the aspect ratios, inversion height to source radius and inversion height to radius of the computational region.

The results show the formation of a convective cell above the edge of the heat source which, by virtue of its dynamic pressure field, traps a volume of almost stagnant, almost isothermal air over the centre of the source. Unlike earlier "strip" heat island models the axisymmetric solutions show that the pattern of circulating flow is no longer symmetrical about the source perimeter and further that there is an appreciable difference in the strength of the circulation as the source radius is varied.

P. G. Williams, Monash University

1. INTRODUCTION

It is now well accepted that a city or town generates what is known as an urban heat island, a temperature excess relative to surrounding rural areas. Its existence has been documented for over a century, Howard (8), and more recently heat island climatologies have been established for a number of cities (Duckworth and Sandberg (6); Chandler (3), Mitchell (11); Bornstein (2); Clarke (4)). Little is gained from reviewing these in detail as their results apply to particular localities. There are, however, certain general heat island characteristics that occur in the observations:

(1) the daytime urban temperature excess is generally less than the nocturaal temperature excess
(2) both meteorological and physical factors (e.g. city size) affect heat island intensity
(3) nocturnal inversions above a city occur less frequently than over rural areas
(4) a calm, clear atmosphere produces a stronger nocturnal heat island.

It should be noted that some authors define a heat island solely as the ground level temperature excess whereas others define it as being the whole convective system above the source. As we are here concerned with a dynamical model the latter definition will be used.

A number of mathematical models have been formulated in an attempt to explain quantitatively the above characteristics. Myrup (12) produced an energy budget model in an attempt to identify quantitatively the various contributions to the heat source. From this he concluded that reduced evaporation in urban areas and the thermal properties of urban materials were among the most significant parameters. However, his model predicted that the temperature excess would be less at night than during the day and this is inconsistent with observations. Other models, primarily numerical, seek to elucidate the effect of the heat island on the air flow above the urban area. Delage and Taylor (5) have developed a two-dimensional time-dependent model to simulate wind flow in a vertical cross section of the heat island. The model is derived for a strip heat source, implying a heat island which is infinitely long in one direction and the hydro static approximation is applied to the atmosphere within the computational region. This assumes vertical fluid accelerations are negligible in relation to horizontal fluid accelerations and from their solutions for transient and steady state wind fields it can be shown that this is not so, suggesting that use of the hydrostatic approximation is not well justified. Despite this, their results show that the inward flow of cooler rural air can produce an elevated inversion over the city, with a small cross over effect, both consistent with the observation of Bornstein (2).

Further, they found that an increase in magnitude of the eddy transfer coefficient served to increase the depth of circulation, and that steady state was achieved sooner in this case. Their results indicated that variation in heat island width had no significant effect on the intensity of circulation. However, they did not consider the effect of the lateral boundary condition on circulation to determine whether or not sufficient freedom for flow had been allowed across this boundary.

A further numerical model by Leslie & Morton (9) was used to investigate convection above a large weak heat source in a region closed by a strong inversion and free of synoptic winds. This model is also two-dimensional with the urban source being specified by its temperature excess above the rural surroundings. Rather than using the hydrostatic approximation to eliminate the equation for vertical momentum, Leslie and Morton use the full equations for horizontal and vertical momentum and apply the Boussinesq approximation. The authors were principally concerned with the convective dependence of the flow on a number of flow parameters, and on the lateral boundary conditions. Their results show the development of a symmetrical, buoyantly driven natural circulation centred above the edge of the heat source. Between this eddy region and the symmetry axis exists a region of almost stagnant air at near source temperature. The authors found that their steady state circulation depended on the flow Rayleigh number, the lateral boundary condition on temperature, and the aspect ratio of inversion height to source half width. Also that the intensity of circulation was unaffected by the size of the heat source for a given inversion height.

These models of convection over "strip" heat islands show the development of a circulating flow above the urban perimeter, the strength of which is relatively unaffected by the size of the heat island. There is, however, some doubt concerning the role of the boundary conditions, particularly at the "open" lateral boundary in determining the character of the solution. The present paper extends results obtained from investigation of "strip" heat islands by considering an axisymmetric configuration. There are two reasons for this, firstly the configuration more nearly represents that of many cities, and more importantly there is a changed relative role of the outer boundary conditions in the axisymmetric configuration.

The model is time-dependent and is designed such as to reproduce broadly the major effects

of convective flow over a low intensity, circular heat source, in the presence of a strong inversion under conditions of negligible wind. A number of numerical experiments were carried out to determine flow dependence on the following flow parameters (i) the Pseudo Rayleigh number, (ii) the two aspect ratios, inversion height to source radius and inversion height to the radius of the computational region, and (iii) the various boundary conditions employed.

2. FORMULATION OF THE MODEL

We start by considering two-dimensional motion above a heated circular region and refer to cylindrical co-ordinates (r,z). The complete equations for momentum, continuity and heat in cylindrical co-ordinates, restricted to an r-z plane, are:

$$\frac{\partial u}{\partial t} + \underset{\sim}{u}.\nabla u = -\frac{1}{\rho}\frac{\partial p}{\partial r} + \frac{1}{\rho}(\rho-\rho_o)\underset{\sim}{g} + K[\nabla^2 u - \frac{u}{r^2}] , \tag{1a}$$

$$\frac{\partial v}{\partial t} + \underset{\sim}{u}.\nabla v = -\frac{1}{\rho}\frac{\partial p}{\partial z} + \frac{1}{\rho}(\rho-\rho_o)\underset{\sim}{g} + K\nabla^2 v, \tag{1b}$$

$$\frac{\partial \rho}{\partial t} + \underset{\sim}{u}.\nabla\rho = \rho\nabla.\underset{\sim}{u}, \tag{2}$$

and

$$\frac{\partial T}{\partial t} + \underset{\sim}{u}.\nabla T = K\nabla^2 T , \tag{3}$$

where u and v are velocity components in the r and z directions respectively, $g = (0,-g)$ is the acceleration due to gravity, P is dynamic pressure and K a turbulent eddy diffusivity. The eddy diffusivity is assumed constant the isotropic over the computational region and equal for both momentum and heat.

By making use of potential temperatures and densities to allow for hydrostatic changes in pressure, density changes will be small for the relatively weak convective fields studied, and primarily associated with temperature changes. Thus we make the Boussinesq approximation which assumes that changes in density are important only in the buoyancy term of the momentum equations and we may take Charles' Law as the approximate equation of state, i.e.

$$\rho T = \rho_o T_o \tag{4}$$

where ρ_o is the initial uniform density of the region prior to motion commencing and T_o is the initial uniform temperature.

Using the equation of state where appropriate and expanding, equations (1a), (1b), (2) and (3) become:

$$\frac{\partial u}{\partial t} + u\frac{\partial u}{\partial r} + v\frac{\partial u}{\partial z} = -\frac{1}{\rho_o}\frac{\partial p}{\partial r} + K[\frac{\partial^2 u}{\partial r^2} + \frac{1}{r}\frac{\partial u}{\partial r} + \frac{\partial^2 u}{\partial z^2}], \tag{5a}$$

$$\frac{\partial v}{\partial t} + u\frac{\partial v}{\partial r} + v\frac{\partial v}{\partial z} = -\frac{1}{\rho_o}\frac{\partial p}{\partial z} + (\frac{T-T_o}{T_o})g + K[\frac{\partial^2 v}{\partial r^2} + \frac{1}{r}\frac{\partial v}{\partial r} + \frac{\partial^2 v}{\partial z^2}], \tag{5b}$$

$$\frac{\partial}{\partial r}(ru) + r\frac{\partial v}{\partial z} = 0 , \tag{6}$$

and

$$\frac{\partial T}{\partial t} + u\frac{\partial T}{\partial r} + v\frac{\partial T}{\partial z} = K[\frac{\partial^2 T}{\partial r^2} + \frac{1}{r}\frac{\partial T}{\partial r} + \frac{\partial^2 T}{\partial z^2}] . \tag{7}$$

Equations (5a), (5b), (6) and (7) form a closed set and may now be used to determine the convective fields of pressure temperature and velocity given suitable initial and boundary conditions.

3. INITIAL AND BOUNDARY CONDITIONS

The heat source is taken within the circular region $0 \leq r \leq \ell$, $z=0$ and has a source temperature, T_s, in excess of the initial ambient temperature T_o of the fluid and the constant outer ground temperature T_o. Motion is symmetrical about $r=0$ within a vertical plane through the heat source and is constrained by the inversion at $z=H$ and the ground at $z=0$. Figure 1 shows the computational region.

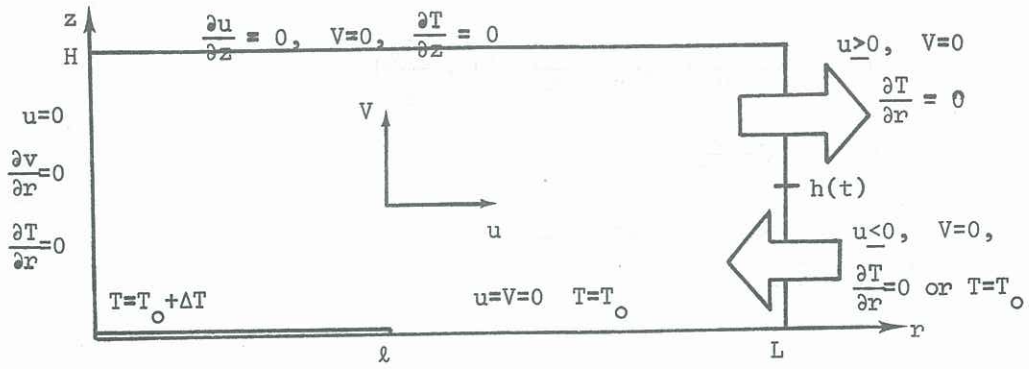

Figure 1: computational region and Boundary Conditions.

The boundary conditions on $(r = 0, 0 \leq z \leq H)$ express symmetry and are $u = 0$, $\frac{\partial v}{\partial r} = 0$, and $\frac{\partial T}{\partial r} = 0$.

On the lower boundary (ground level), the no-slip condition is represented as $u = v = 0$ and

$$T = \begin{cases} T_o + \Delta T & 0 \leq r \leq \ell \\ T_o & \ell < r \leq R \end{cases}.$$

Upper boundary conditions $(0 \leq r \leq R, z = H)$, are $\frac{\partial u}{\partial z} = 0$, $v = 0$ and $\frac{\partial T}{\partial z} = 0$. These may be thought of as modelling a strong inversion through which flow is unable to penetrate and assumes no tangential stress and no vertical heat flux at $z = H$. Such assumptions are consistent with the expectation that the degree of heat or momentum transport across the inversion will not be great enough to cause significant effects to the flow within the region.

Conditions on the lateral boundary, $(r = R, 0 \leq z \leq H)$ are chosen such as to permit inward flow below some height, $h(t)$, and a venting outflow between $h(t)$ and the inversion at H. The flow reversal height $h(t)$ is determined from

$$\int_0^H u(R,z)dz = 0,$$

which represents (in the Boussinesq approximation) conservation of mass flux over the entire lateral boundary. The thermal boundary condition for the outflow region, $h(t) \leq z \leq H$, is taken as $\frac{\partial T}{\partial r} = 0$. This ensures that heat flux is conserved across the boundary in a region where advection should be the dominant mode of heat transport. For the inflow region, $0 \leq z \leq h(t)$, two alternative thermal boundary conditions have been applied. These are that heat flux is conserved, i.e. $\frac{\partial T}{\partial r} = 0$, or that the incoming flow has the local environmental temperature $T = T_o$. It is expected that appreciable differences may result except in the advective dominated solutions, being there at higher values of the pseudo-Rayleigh number.

As there is no imposed velocity scale, motion is induced solely by buoyancy forces and thus the pseudo-Rayleigh number,

$$Ra = \frac{g\Delta TH^3}{K^2T_o},$$

defined in terms of the turbulent eddy diffusivity K, excess temperature ΔT and height of the computational region H, is the only dynamical parameter involved. The other characteristic parameters of the flow are the two aspect ratios, H/ℓ and H/L, which define the geometry of the convective system and computational region respectively.

4. NUMERICAL PROCEDURE

The number of dependent variables in the system may be reduced by the introduction of a stream function ψ and a zonal vorticity component ζ, defined by

$$u = -\frac{1}{r}\frac{\partial\psi}{\partial z}, \quad v = \frac{1}{r}\frac{\partial\psi}{\partial r}, \tag{8}$$

and

$$\zeta = \frac{\partial u}{\partial z} - \frac{\partial v}{\partial r}. \tag{9}$$

By use of equations (8) and (9), it may be shown that the set of equations (5a), (5b) and (6) reduce to

$$\frac{D\zeta}{Dt} = \frac{\partial\zeta}{\partial t} + J(\psi,\frac{\zeta}{r}) = -\frac{g}{T_o}\frac{\partial T}{\partial r} + K[\frac{\partial}{\partial r}(\frac{1}{r}\frac{\partial}{\partial r}(r\zeta)) + \frac{\partial^2\zeta}{\partial z^2}] \tag{10}$$

$$\frac{DT}{Dt} = \frac{\partial T}{\partial t} + \frac{1}{r}J(\psi,T) = K[\frac{1}{r}\frac{\partial}{\partial r}(r\frac{\partial T}{\partial r}) + \frac{\partial^2 T}{\partial z^2}] \tag{11}$$

together with a diagnostic equation for ψ,

$$-\zeta = \frac{\partial}{\partial r}(\frac{1}{r}\frac{\partial\psi}{\partial r}) + \frac{1}{r}(\frac{\partial^2\psi}{\partial z^2}) \quad . \tag{12}$$

The Jacobian notation,

$$J(\mu,\nu) = \frac{\partial\mu}{\partial r}\frac{\partial\nu}{\partial z} - \frac{\partial\mu}{\partial z}\frac{\partial\nu}{\partial r}$$

has been used to express the convective parts of the total derivations $\frac{D\zeta}{Dt}$ and $\frac{DT}{Dt}$.

It is now necessary to replace the set of differential equations (10), (11) and (12) by an appropriate set of finite difference analogues defined on a uniform mesh in the (r,z) plane at times $\eta\Delta t(\eta=0,1,2\ldots)$. The finite differencing scheme employed is:

$$\delta_t\bar{\zeta}^t + J_a(\psi,\frac{\zeta}{r}) = \frac{-g}{T_o}\delta_r\bar{T}^r + K[\zeta^*_{rr} + \frac{1}{r}\delta_r\bar{\zeta}^r - \frac{\zeta}{r^2} + \zeta^*_{zz}], \tag{13}$$

$$\delta_t\bar{T}^t + \frac{1}{r}J_b(\psi,T) = K[T^*_{rr} + \frac{1}{r}\delta_r\bar{T}^r + T^*_{zz}], \tag{14}$$

and

$$-\zeta = \frac{1}{r}\delta_{zz}\psi + \delta_r(\frac{1}{r}\delta_r\psi) \tag{15}$$

where $\bar{\beta}^r = \frac{1}{2}[\beta(r+\frac{\Delta r}{2}) + \beta(r-\frac{\Delta r}{2})]$ and $\delta_r\beta = \frac{1}{\Delta r}[\beta(r+\frac{\Delta r}{2}) - \beta(r-\frac{\Delta r}{2})]$

are respectively the averaging and differencing operators as defined by Lilly (10). The operator

$$\beta^*_{rr} = \frac{\beta^n_{i+1j}+\beta^n_{i-1j}-\beta^{n+1}_{ij}-\beta^{n-1}_{ij}}{(\Delta r)^2}$$

employs the method of Dufort and Frankel (7) in providing an explicit method for removing the diffusive time step requirement, thus allowing for smaller time steps to be used in the numerical solutions. The Jacobian difference operators

$$J_a(\psi,\frac{\zeta}{r}) = \frac{1}{3}[2J_b(\psi,\frac{\zeta}{r}) + \delta_r(\overline{\psi\delta_z(\frac{\bar{\zeta}}{r})^z})^r - \delta_z(\overline{\psi\delta_r(\frac{\bar{\zeta}}{r})^r})^z)] \ ,$$

and

$$J_b(\psi,T) = \delta_z(\bar{T}^z\delta_r\bar{\psi}^{rz}) - \delta_r(\bar{T}^r\delta_z\bar{\psi}^{rz})$$

were devised by Arakawa (1) in order to overcome certain non-linear instabilities in the finite difference analogues to the differential equations.

The numerical procedure itself consists of successively solving equations (13), (14) and (15) until the required state of flow development, generally the steady state, is achieved. Solution of equations (13) and (14) is straightforward as these are merely evolution equations whilst the vorticity-stream function equation, (14) is solved by successive over relaxation.

5. RESULTS

In all, sixteen numerical experiments were conducted to investigate fully the effects of the flow parameters cited in Section 1. Space limitations restrict us to only a brief, general account here and a broader discussion, considering both the transient solutions and the effect of the various parameters, will be given at the Conference.

Convective motion is initiated in all of the experiments by having the computational region at 300°K and then raising the source temperature to 302°K, this excess being maintained. The results shown in figure 2 show the pattern of steady state streamlines and isotherms for the case where the source aspect ratio $H/\ell=\frac{1}{2}$ and the computational region aspect ratio $H/L = \frac{1}{6}$ with Ra = 3800. Although not illustrated here, motion commences in the form of a starting plume which rises and vents beneath the inversion and as low-level winds develop towards the heat island centre, advection of colder air displaces the horizontal temperature gradients towards the centre. In the early stages of flow development a reverse cell, located above the

inner region of the source, is noticeable but as the inflow continues to penetrate from the edge of the heat island this cell vanishes. The formation of this reverse cell is a consequence of the step change in temperature at the edge of the source and the numerical techniques employed; and seems not representative of any real atmospheric event. As time passes the buoyancy forces in the region between the convective cell and the symmetry axis progressively decrease as the temperature of the region becomes more uniform. At the same time the temperature of the convective cell increases and this behaviour continues until a steady state situation is achieved. In the steady state streamline pattern, figure 2a, the column of less dense air above the central part of the source is maintained dynamically by the circulating flow above the city perimeter.

Due to the axisymmetric configuration there is a relative divergence of the computational region as radius increases. The circulating motion is induced relative to the temperature diffurence at the source radius and this means that flow in the exterior region $\ell < r \leq L$, will experience less lateral restraint than does the fluid in the interior region $0 < r \leq \ell$. As a result the circulating flow produced is not symmetrical about the source perimeter, as is the case with "strip" heat islands, but in elongated radially outward with a consequent displacement of the horizontal temperature gradients (figures 2a, 2b).

Figure 3 shows the steady state results for a case which differs only in that the aspect ratio $H/\ell = \frac{1}{4}$, thus giving a larger heat source relative to both the inversion height and the radius of the computational region. Again the resulting circulation is located above the source perimeter and is non-symmetric.

It may be shown that the heat conducted through the lower boundary varies with radius and is greatest near the source perimeter and that in this case, the heat flux per radian in the region of the perimeter is given by:

$$\text{Heat Flux/Radian} \approx k r_m \Delta r,$$

where k is thermal conductivity, Δr is the radial grid spacing, r_m is the mean source radius and the vertical temperature gradient at the ground kevel is taken as one in this region. From this it can be seen that doubling the source radius will approximately double the heat flux/radian in this region which gives a consequent doubling to the strength of the maximum stream function, as shown in figures 2a and 3a.

In the case of the "strip" heat island the distance between the edge of the source and the edge of the computational region had little effect on the results. Solution from the axisymmetric model show that the strength of circulation in the outer region is affected as ℓ/L is altered, due to the changed relative role of the outer boundary conditions which now exhibit less lateral constraint on the flow.

In conclusion it should be noted that due to several limiting assumptions these solutions cannot represent the full complexity of real atmospheric urban-rural convection. The temperature excess found in real citieshas a diurnal cycle, the cities are often ventilated by external winds, and the low level wind fields are affected by the buildings within the urban area. However the development of the region of stagnant air, held in position by the pressure field of the circulating flow is applicable to real situations. As the temperature excess ultimately induces this stagnant region the retention of "green belts" within the urban area would seem a desirable situation, promoting evaporation and thus reducing the urban temperature excess. However the already intensive urbanisation of many cities may mean that further development would be less climatically signficaant as new urban structures tend to replace old ones rather than encroaching on already limited urban green areas.

ACKNOWLEDGEMENTS

This work was conducted under the direction of Professor B. R. Morton, Department of Mathematics, Monash University, and the author wishes to gratefully acknowledge the State Electricity Commission of Victoria for their financial support and Dr. R. A. Pearson for his assistance with the numerical techniques.*

REFERENCES

(1) Arakawa, A. (1966) "Computational Design of Long-term Numerical Integration of the Equations of Fluid Motion: I. Two-dimensional Incompressible Flow". J.Computational Physics, 1 , 119.

(2) Bornstein, R. D. (1968) "Observations of the Urban Heat Island Effect in New York City". J.Appl.Meteor., 7 , 575.

(3) Chandler, T. J. (1962) "London's Urban Climate". Geography J., 127 , 279.

(4) Clarke, J. F. (1968) "Nocturnal Urban Boundary Layer over Cincinnati Ohio". Monthly Weather Review, 97(8) , 582.

(5) Delage, Y. & Taylor, P. A. (1970) "Numerical Studies of Heat Island Circulation". Boundary-layer Meteorology, 1 , 201.

(6) Duckworth, F. S. & Sandberg,J.S.(1954) "The Effect of Cities upon Horizontal and Vertical Temperature Gradients". Bull.Am.Meteor.Soc., 35(5) , 198.

(7) Dufort, E. C. and Frankel, S. P. (1953) "Stability Conditions in the Numerical Treatment of Parabolic Differential Equations". Math.Tables and Other Aids to Computation, 7 , 135.

(8) Howard, L. (1833) "The Climate of London Deduced from Meteorological Observations". 3rd Edition, Harvey and Daton London.

(9) Leslie, L. M. and Morton, B. R. (1973) "Convective Stagnation under an Inversion--A Numerical Experiment". Proc.First Australasian Conf. on Heat & Mass Transfer, Monash University, Melbourne, May 1973.

(10) Lilley, D. K. (1964) "Numerical Solutions for the Shape-preserving Two-dimensional Thermal Convection Element". J.Atmos.Sci., 21 , 83.

(11) Mitchell, J. M. (1961) "The Temperature of Cities". Weatherwise, 14 , 224.

(12) Myrup, L. O. (1969) "A Numerical Model of the Urban Heat Island". J.Appl.Meteor., 8(6) , 908.

*Dr. Pearson has been supported by an A.R.G.C. Grant.

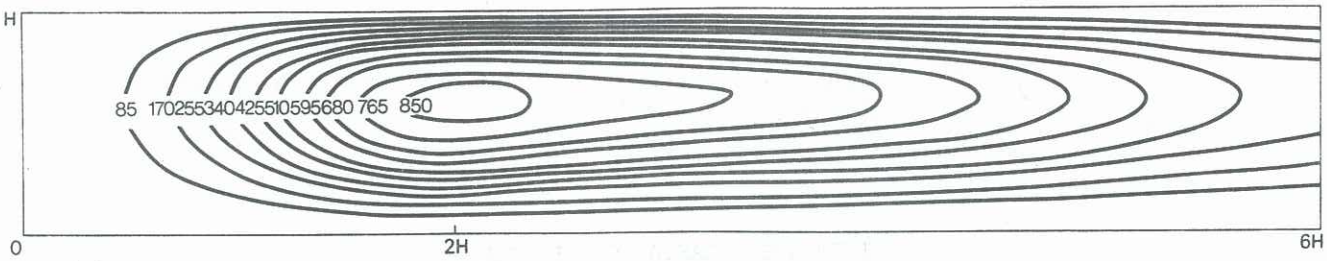

(a) Streamlines contours vary from 0.0 to 8.5×10^5 m^3/sec. Scaled by 1.0×10^{-3}.

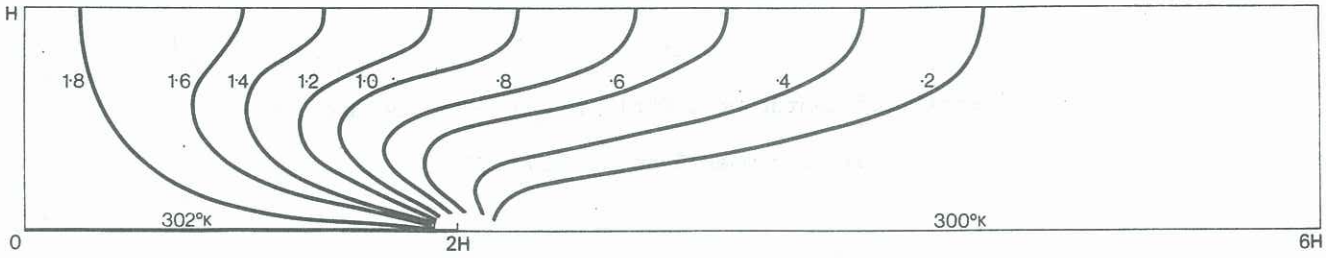

(b) Isotherms contours vary from 300.2 to 301.8°K.

Figure 2: steady state results for case with Ra=3800, $H/\ell=\frac{1}{2}$, $H/L=\frac{1}{6}$, $T=T_o$ for inflow boundary.

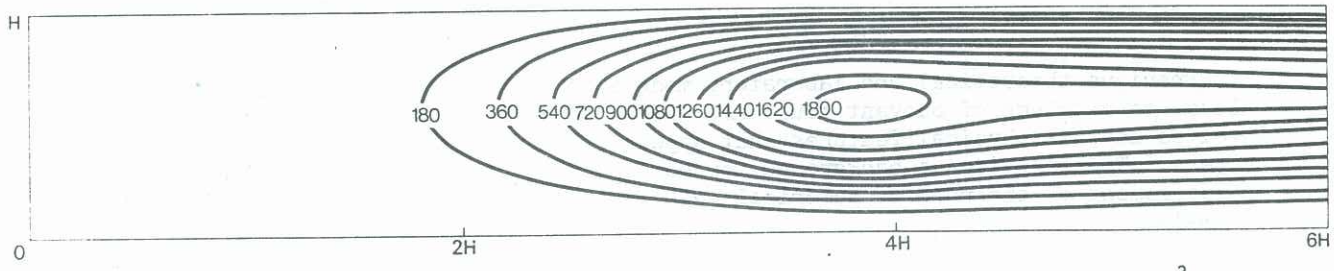

(a) Streamlines contours vary from 0.0 to 1.8×10^6 m^3/sec. Scaled by 1.0×10^{-3}.

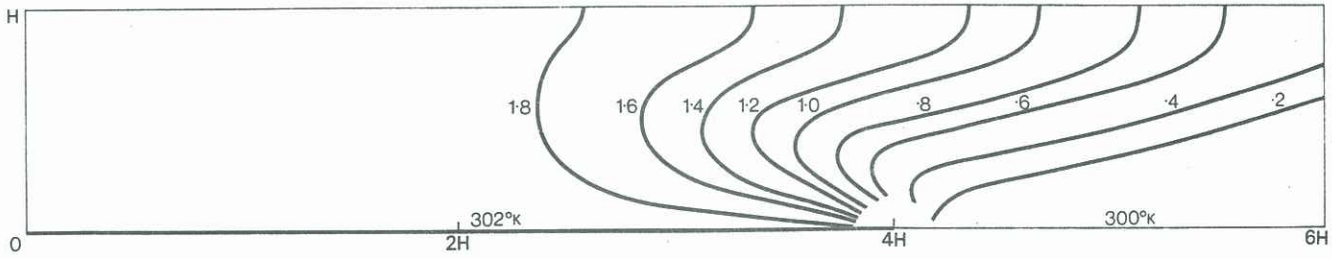

(b) Isotherms contours vary from 300.2 to 301.8°K.

Figure 3: steady state results for case with Ra=3800, $H/\ell=\frac{1}{4}$, $H/L=\frac{1}{6}$, $T=T_o$ for inflow boundary.